CHIN. PHYS. LETT. Vol. 29, No. 11 (2012) 118502

Structural Design of a Compact in-Plane Nano-Grating Accelerometer *

YAO Bao-Yin(姚保寅)**, ZHOU Zhen(周震), FENG Li-Shuang(冯丽爽),
WANG Wen-Pu(王文璞), WANG Xiao(王潇)

Key Laboratory of Micro-nano Measurement-manipulation and Physics (Ministry of Education), Beihang University, Beijing 100191

Fundamental of Science on Novel Inertial Instrument & Navigation System Technology Laboratory, Beihang University, Beijing 100191

(Received 9 July 2012)

A combination of large mass, weak spring and nano-grating is the key for a nano-grating accelerometer to measure nano-G acceleration. A novel compact nano-grating accelerometer integrating a large mass with nano-grating is proposed. First, the numbers of diffraction orders are calculated. Then, structure parameters are optimized by finite element analysis to achieve a high sensitivity in an ideal vibration mode. Finally, we design the fabrication method to form such a compact nano-grating accelerometer and successfully fabricate the uniform and well-designed nano-gratings with a period of 847 nm, crater of 451 nm by an FIB/SEM dual beam system. Based on the ANSYS simulation, a nano-grating accelerometer is predicted to work in the first modal and enables the accelerometer to have displacement sensitivity at 197 nm/G with a measurement range of ±1 G, corresponding to zeroth diffraction beam optical sensitivity 1%/mG. The nano-gratings fabricated are very close to those designed ones within experimental error to lay the foundation for the sequent fabrication. These results provide a theoretical basis for the design and fabrication of nano-grating accelerometers.

PACS: 85.85.+j, 87.85.Qr, 42.79.Dj DOI: 10.1088/0256-307X/29/11/118502

Recently nano-grating accelerometers have generated considerable interest in the scientific community due to their wide variety of advantages, such as immunity to electromagnetic interference, electrical insulating, corrosion-resistance, remote sensing, extremely high-sensitivity and multiplexing ability. They are based on near-field optics using a two layer sub-wavelength grating with a wide range of applications in highly precise navigation, vibration sensing of vehicles, seismic sensing and oil-field applications.[1]

Sub-wavelength (SW) gratings have periods shorter than the wavelength of the incident illuminating source. They modulate the near-field intensity and polarization of an incident light source in response to the relative lateral motion of the two sub-wavelength gratings (shown in Fig. 1). Sometimes, electrostatic actuators are integrated into a sensor to control nano-grating motion to characterize the displacement sensitivity.

As for the fabrication of nano-gratings, an FIB/SEM dual beam has many advantages including in-situ observations, relatively high resolution and efficiency compared with other processing methods.[2–6]

Keeler *et al.*[7] demonstrated electrostatically stretching SW gratings for inertial sensing applications. Krishnamoorthya designed the integrated sub-wavelength optical nano-grating accelerometers with device sensitivities of 590 V/G and noise floors corresponding to 17 nG/$\sqrt{\text{Hz}}$ (at 1 Hz).[1] However, to our knowledge, the overall structure is complicated. The mechanical structure and nano-grating are made separately, which makes the fabrication difficult. In this study, we integrate the large mass, weak spring and sub-wavelength grating together. Design and simulation of the overall structure are made with Ansys. The novel nano-grating accelerometer was finally designed with displacement sensitivity 197 Hz/G. An FIB/SEM dual beam system was used to fabricate the nano-gratings without a mask which can make the structure and fabrication simpler with a good grating profile.

The concept of a novel nano-grating accelerometer is shown in Fig. 2. It consists of two sets of polysilicon sub-wavelength gratings separated by an air gap, large mass, four weak folded springs.

When illuminated by plane waves, there are no visible diffraction orders observed in the far field. However, in the near field, there are non-propagating waves that are bound to the surface. If a second sub-wavelength grating is brought into close proximity (∼0.6 μm) to the first one, re-propagation of the evanescent energy into propagating waves can be accomplished. Relative displacement between these two sets of sub-wavelength gratings can result in changes of the effective index of the overall structure. The reflected/transmitted optical beam intensity from the nano-gratings is measured as a function of the relative lateral positions of the nano-gratings. Such a kind of optical sensor has extremely high optical sensitivity

*Supported by the National Natural Science Foundation of China under Grant No 60908016.
**Corresponding author. Email: yaobaoyin123@163.com; yaobaoyin123@gmail.com
© 2012 Chinese Physical Society and IOP Publishing Ltd

that can be 5%/nm.[8]

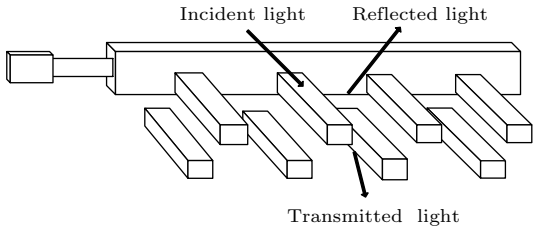


Fig. 1. Deformable nano-grating structure.

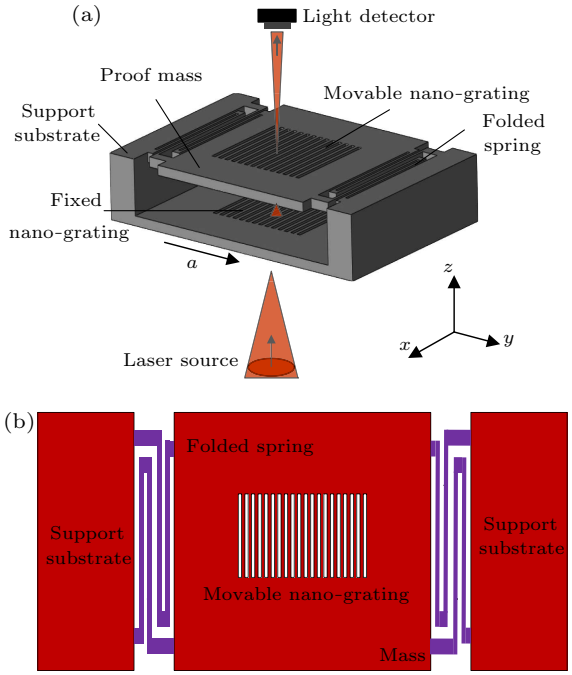


Fig. 2. Schematic of nano-grating accelerometer: (a) overall structure of nano-grating accelerometer, (b) top view of nano-grating accelerometer.

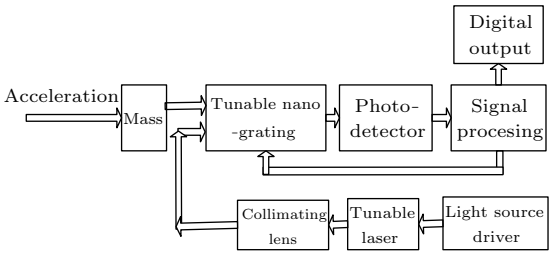


Fig. 3. Scheme of the system.

The nano-grating accelerometer system consists of several parts, including the mass, nano-grating, light source, photo-detector and demodulation circuit, as shown in Fig. 3. The open loop system was chosen for simplicity in the initial design. The closed loop system will be used in a future design.

The main challenges in building such a system include integrating the large mass with a weak spring and nano-gratings with a high depth/width ratio. Then, its sensitivity can reach as high as 10^{-9} G.

A linearly polarized electromagnetic wave is incident at an arbitrary angle of incidence of α and azimuthal angle of β upon a binary dielectric grating (shown in Fig. 4) with period d, width a and depth h. The grating is bound by two different media with refractive indices $n_{\rm I}$ and $n_{\rm III}$. Regions I and III correspond to the incidence and transmission region. The normal to the boundary is in the z direction, and the grating vector is in the y direction.[9]

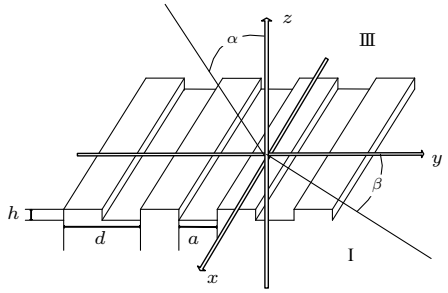


Fig. 4. Geometry of the nano-grating diffraction.

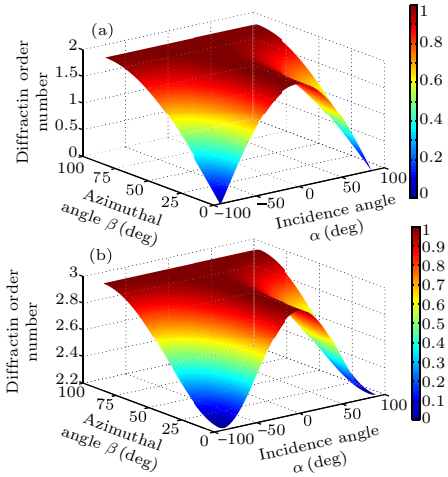


Fig. 5. Diffraction order number versus incidence angle with azimuthal angle (a) $n_{\rm I} = 1$, $n_{\rm III} = 1$, (b) $n_{\rm I} = 1$, $n_{\rm III} = 1.5$.

In our design, the grating period and incident light wavelength are 840 nm and 850 nm, respectively. There are in total 20 periods and each grating is designed with a thickness of 830 nm. The gap between the two layers is 400 nm. According to the diffraction theory, we can obtain the diffraction orders number m in the following equations:

$$m = \frac{2d}{\lambda}\sqrt{n_p^2 - (n_{\rm I}\sin\alpha\cos\beta)^2},\ p = {\rm I}, {\rm III}. \quad (1)$$

We can obtain the relationship between the diffraction order number (region III) and the incidence angle with the azimuthal angle (shown in Fig. 5).

Seen from the graph, when the incident angel is 0°, the diffraction orders in the transmission region are greatest. In our design, both regions I and III are air, the azimuthal angle is 90°. We can only obtain the zeroth diffraction beam.

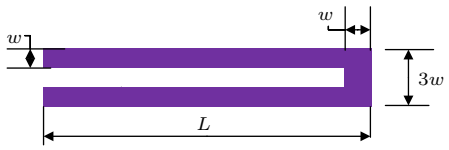


Fig. 6. Simplified model of the folded spring.

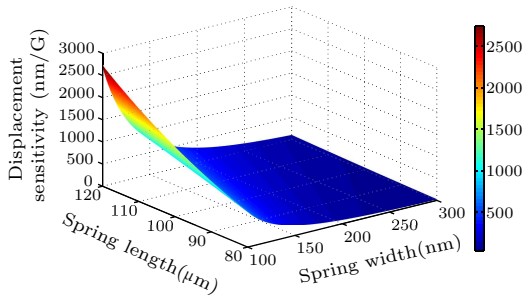


Fig. 7. Displacement versus spring length and width.

According to the rigorous coupled wave analysis, we obtain that the diffraction efficiency can be given similarly to the literature.[10]

The acceleration experienced by this proof mass is directly proportional to its displacement as shown in the equation

$$a = w_0^2 x = \frac{k}{m} x, \tag{2}$$

where a is the acceleration experienced by the proof mass, x is its displacement, w_0 is the resonant frequency of the proof mass, k is its mechanical spring constant, and m is its mass.

We can measure nano-G acceleration, displacement sensitivities in the femto-meter scale, low resonant frequencies, large mass and a weak spring constant k based on Eq. (1).

Considering the fabrication, spring height is the same as that of mass and should not be too deep. Additionally, due to the high sensitivity of our device, the folded springs are used to provide isolation of higher frequency inputs and the mass with an optical sensor from the thermally induced stresses caused by the mismatch. The folded spring can be simplified as shown in Fig. 6.

Based on Ref. [11], the stiffness constant of the four folded springs can be obtained. The equation is

$$\frac{1}{k_e} = \frac{1}{Et}\left(\frac{L^3}{2w^3} + \frac{3(1+\mu)L}{5w} + \frac{3w}{4w} - \frac{3L^*(3w)^2}{4w^3}\right), \tag{3}$$

where E is Young's modulus, μ is Poison's ratio, L, t and w are the length, thickness and width of the suspension beam, respectively.

Based on Chae *et al.*,[12] the stiffness constant of a folded spring can be given by

$$k_e \approx \frac{24E}{L^3}\left(\frac{h \cdot w^3}{12}\right) = \frac{2Ehw^3}{L^3}. \tag{4}$$

The masses of the spring and the gratings are so small to be ignored. The equations that define the springs for the device are given as follows: effective spring constant in the y direction reads

$$k_y = k_e = \frac{2Ehw^3}{L^3}, \tag{5}$$

effective spring constant in the x direction is

$$k_x = \frac{8Ehw}{L}, \tag{6}$$

effective spring constant in the z direction is

$$k_z = \frac{2Ewh^3}{L^3}, \tag{7}$$

displacement sensitivity of the accelerometer reads

$$s = \frac{x}{a} = \frac{\rho b^2 L^3}{2Ew^3}, \tag{8}$$

the resonant frequency is

$$f = \frac{1}{2\pi}\sqrt{\frac{2Ew^3}{\rho b^2 L^3}}, \tag{9}$$

where b is the width of the mass.

The ratios of spring constants for the mass are

$$\frac{k_x}{k_y} = \frac{4L^2}{w^2}, \tag{10}$$

$$\frac{k_z}{k_y} = \frac{h^2}{w^2}. \tag{11}$$

Considering fabrication of the accelerometer, the thickness of the spring is chosen to be 400 nm. The relationships of displacement sensitivity to spring width and length can be obtained when b equals 150 μm. The relationship between displacement sensitivity and structure parameters are shown in Fig. 3.

From Fig. 7, we can see that a longer and narrower supporting beam can improve sensor sensitivity. Considering cross axis sensitivity, the spring width should not be larger than thickness. They should be controlled properly. There is no relationship between the thickness and sensitivity. The sensor structure size in this study is finally designed as follows: folded supporting beams in length 100 μm, in width 0.2 μm and in thickness 0.4 μm. The width and thickness of the mass is 150 μm and 0.4 μm, respectively. From the above equations, we can obtain that the designed sensor sensitivity and resonant frequency respectively as shown in the following:

$$s = \frac{x}{a} = \frac{\rho b^2 L^3}{2Ew^3} = 198\,\text{nm/G},$$

$$f = \frac{1}{2\pi}\sqrt{\frac{2Ew^3}{\rho b^2 L^3}} = 1120\,\text{Hz}.$$

The ratios of the spring constants for the mass, $\frac{k_x}{k_y}$ and $\frac{k_z}{k_y}$, are 10^6 and 4, respectively. Hence, this design

should provide adequate decoupling between modes in the x, y and z directions for the device.

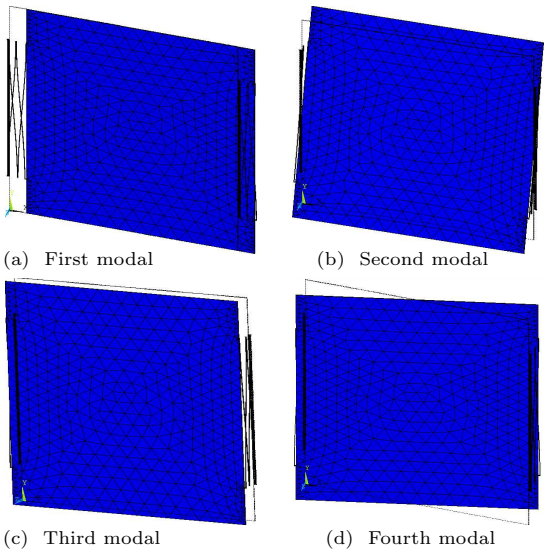


Fig. 8. Modals of the accelerometer with ANSYS: (a) first modal, (b) second modal, (c) third modal, (d) fourth modal.

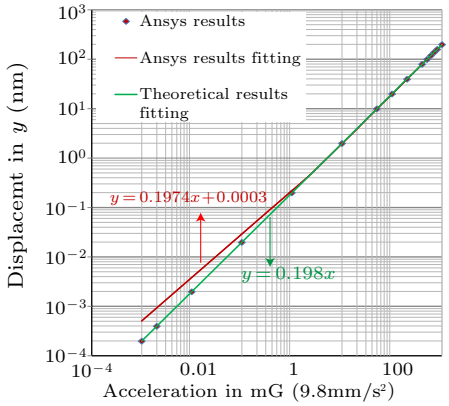


Fig. 9. Displacement sensitivity simulated with Ansys with results corresponding to the theoretical value.

According to the literature, the optical sensitivity of the nano-grating accelerometer can reach 5%/nm. This translates the accelerometer sensitivity to 1%/mG.

A finite element model for this spring-mass model is developed using Ansys. Modal simulations predicted dominant resonant frequencies at 1122 Hz (y translation of mass) corresponding to the calculated value 1120 Hz. The deviation between the calculated value and the simulated value is only 0.18%. Figure 8 and Table 1 outline the modals of the accelerometer and the resonant frequencies respectively.

From the simulation, we can see that only the first modal is the in-plane modal we need, in comparison to other three out-plane modals.

As for the sensitivity, we apply different accelerations to the mass, and the displacement versus acceleration relationship is simulated (Fig. 9). It can be seen that the displacement sensitivity s simulated with Ansys is 197.4 nm/G, which fits the theoretical results 198 nm/G very well. The stress distribution under 1 G acceleration is also obtained (Fig. 10). We can see that the stress in the joint between the mass and folded springs is the largest.

Table 1. Resonant frequencies of the modals.

Modal	Resonant frequency (Hz)
1	1122.3 (Working modal)
2	1475.7
3	2169.5
4	3885.0

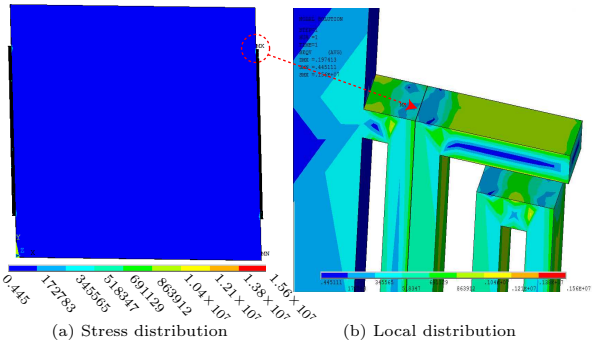


Fig. 10. Stress distribution of accelerometer under 1 G (9.8 m/s^2) acceleration: (a) stress distribution, (b) local distribution.

Seen from Fig. 8, the largest stress is in the joint between mass and the folded spring, 1.56 MPa, much less than the utmost stress of silicon, 70 MPa. The spring has reached its structure limit. Hence the measurement range is ±1 G.

Considering the integration of VCSEL (850 nm) illuminating source, nano-graing optical sensor, detector etc. and relative optical simulation, the period, width and thickness of the optical gratings we chose are 840 nm, 415 nm and 400 nm, respectively. The FIB/SEM dual beam system has many advantages including in-situ observation, relatively high resolution and efficiency. It is used to fabricate the two sets of nano-gratings with an air gap of 400 nm.

The silicon wafers were patterned and etched from the backside. The oxide layer under the nano-gratings provides an etch-stop for the DRIE silicon etch. The FIB/SEM dual beam etch must be optimized to ensure uniform etching of the springs and through-wafer vias with target aspect ratios >1:18. This is followed by a hydrofluoric acid (HF) dip to remove buried oxide layers and to release the optical sensors. Finally, a CO_2 supercritical drying step is used to prevent stiction of the fragile nano-gratings to the substrate. Figure 11 outlines the fabrication process for both the optical sensors and the integrated proof mass.

We fabricate the uniform and well-designed nano-grating with period of 840 nm, crater of 425 nm by the FIB/SEM dual beam system (Fig. 12).[13]

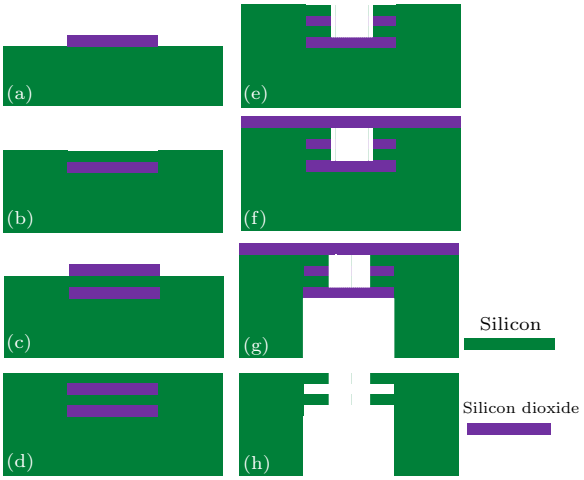


Fig. 11. Schematic process flow of the nano-grating accelerometer device: (a) deposit oxide isolation layer (2 μm), (b) deposit and pattern first polysilicon layer (0.4 μm), deposit and pattern first sacrificial oxide layer (0.4 μm), (d) deposit and pattern second polysilicon layer (0.4 μm), (e) pattern nano-gratings and the folded springs with FIB/SEM dual beam system, (f) deposit a second sacrificial oxide layer (2 μm) to protect structures, (g) grind and polishing backside followed by patterning channel for the illuminating source, (h) remove buried oxide layers and release the optical sensors.

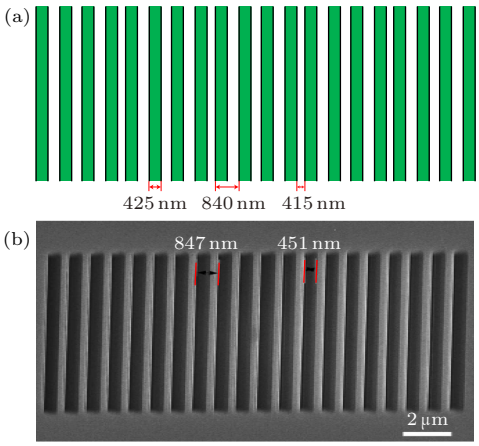


Fig. 12. Image of nano-gratings with (a) designed by graphics generator, the green is crater; (b) SEM image of the fabricated item by FIB, with a period of 847 nm, 451 nm and 396 nm for the crater and hillock separately.

By adjusting the FIB parameters of milling like beam current, dwell time and scanning model, the fabricated nano-gratings are uniform in width and the side wall has a good verticality. We finally obtain the nano-gratings with better regularity and period consistency, which lays a sound foundation for sequent fabrication.

The compact structure of a nano-grating accelerometer with a nano-gratings optical sensor in the mass has been proposed. Compared with the former structures, it is much simpler and more compact. It is demonstrated with displacement sensitivity 197.4 nm/G, resonant frequency 1120 Hz and measurement range ±1 G. As a sub-wavelength grating accelerometer, the optical sensitivity is predicted to be 1%/mG by detecting the zeroth order diffraction beam. The inherent weakness of such a kind of optical sensor is its fabrication especially when the structure is released by HF due to the weak spring and narrow air gap. Stress should be reduced as possible to prevent gratings from sticking to the substrate. Additionally, it is also inherently susceptible to random accelerations during routine handling. Careful packaging and handling are critical and necessary in improving its robustness. Fabrication methods for such a kind of accelerometer are proposed. Nano-gratings with a period of 840 nm and a crater of 425 nm showing good regularity and period consistency are fabricated by an FIB/SEM dual beam system successfully. This can provide a good reference for the design and fabrication of the nana-graing accelerometer. Future research work will focus on optimizing the fabrication parameters to finish the overall device.

References

[1] Krishnamoorthy U, Olsson I I I R H, Bogart G R, Baker M S, Carr D W, Swiler T P and Clews P J 2008 *Sens. Actuat.* A **145** 283
[2] Contreras A M, Grunes J Yan X M, Liddle A and Somorjai G A 2005 *Catal. Lett.* **100** 115
[3] Kato F, Fujinawa S Li Y G and Sugiyama S 2007 *Microsyst. Technol.* **13** 221
[4] Fok L M Liu Y H and Li W J 2010 *IEEE Trans. Autom. Sci. Eng.* **7** 49
[5] Dong W Guo X, Wang S Z, Wang Z L and Ming N B 2008 *Chin. Phys. Lett.* **25** 2957
[6] Wu W X, Luo Y H and Cheng X S 2010 *Chin. Phys. Lett.* **27** 094202
[7] Keeler B E N, Carr D W, Sullivan J P, Friedmann T A, Wendt J R and Maxwell J C 2004 *Opt. Lett.* **29** 1182
[8] Carr D W, Sullivan J P and Friedmann T A 2003 *Opt. Lett.* **28** 1636
[9] Carr D W, Bianca E N K, Sullivan J P, Friedmann T A and Wendt J R 2004 *MOEMS Miniaturized Syst.* Ⅳ (Bellingham WA 24–29 January 2004) **5346** 56
[10] Moharam M G, Grann E B and Pommet D A 1995 *J. Opt. Soc. Am.* A **12** 1068
[11] Chi W W, Azid A A and Majlis B Y 2010 *Arch. Mesh* **62** 5 405
[12] Chae J S, Kulah H, Salian A and Najafi K 2000 *Third Annu. Micro/Nanotechnol. Conf.* (Houston Texas 23–28 January 2000) 623
[13] Yao B Y, Luo H, Feng L S, Zhou Z and Wang R M 2011 *Key Eng. Mater.* **483** 66